Eur. Phys. J. A **22**, 241–252 (2004)
DOI 10.1140/epja/i2004-10037-5

THE EUROPEAN PHYSICAL JOURNAL A

The $\nu 9/2[404]$ orbital and the deformation in the A $\sim$ 100 region

W. Urban[1,2,a], J.A. Pinston[1], J. Genevey[1], T. Rząca-Urban[2], A. Złomaniec[2], G. Simpson[3], J.L. Durell[4], W.R. Phillips[4], A.G. Smith[4], B.J. Varley[4], I. Ahmad[5], and N. Schulz[6]

[1] Laboratoire de Physique Subatomique et de Cosmologie, IN2P3-CNRS/Université Joseph Fourier, F-38026 Grenoble Cedex, France
[2] Institute of Experimental Physics, Warsaw University, ul. Hoża 69, PL-00-681 Warszawa, Poland
[3] Institut Laue-Langevin, F-38042 Grenoble Cedex, France
[4] Schuster Laboratory, Department of Physics and Astronomy, University of Manchester, Manchester M13 9PL, UK
[5] Argonne National Laboratory, Argonne, IL 60439, USA
[6] Institut de Recherches Subatomiques UMR7500, CNRS-IN2P3 et Université Louis Pasteur, F-67037 Strasbourg, France

Received: 10 March 2004 / Revised version: 11 May 2004 /
Published online: 9 November 2004 –
Communicated by D. Schwalm

Abstract. A $T_{1/2} = 16(2)$ ns isomeric level, populated in the spontaneous fission of ^{248}Cm, has been found in ^{101}Zr at 941.8 keV in a measurement of prompt γ-rays using the EUROGAM2 array. The level is interpreted as a K-isomer corresponding to the 9/2[404] neutron-hole excitation. The quadrupole moment, $Q_0 = 3.6(4)$ eb, deduced for the new band indicates a large deformation of $\beta_2 = 0.38(4)$, which is produced by a specific shape-coexistence mechanism. This is another observation of the $\nu 9/2[404]$ orbital in the mass $A \sim 100$ region, confirming the presence of the effect reported first in our previous work. The 9/2[404] neutron-hole excitation is also confirmed in the ^{97}Sr nucleus and the deformation $\beta_2 = 0.44(2)$ is determined for this configuration. The properties of the 9/2[404] neutron orbital and its influence on the onset of deformation in the $A \sim 100$ region are discussed.

PACS. 23.20.Lv γ transitions and level energies – 21.60.Cs Shell model – 25.85.Ca Spontaneous fission – 27.60.+j $90 \leq A \leq 149$

1 Introduction

In a study of highly-deformed 11/2[505] neutron-hole states in the lanthanides, Kleinheinz *et al.* [1,2] pointed out that similar strongly-deformed configurations should be observed in the neutron-rich nuclei of the $A \sim 100$ region. It took nearly three decades to find this effect. In a recent work [3] we have reported the first observation of the $\nu(9/2[404])$ orbital in the ^{99}Zr nucleus. In other regions, such hole states have been seen in several neighbouring nuclei [2]. By analogy one expects that the $\nu(9/2[404])$ orbital in the $A \sim 100$ region should be observed in a number of nuclei close to ^{99}Zr. It is important, therefore, to identify another case of the $\nu(9/2[404])$ orbital in the $A \sim 100$ region, to verify the proposed interpretation of the 1038.8 keV isomer in ^{99}Zr as the $K = 9/2$, $9/2^+[404]$ neutron-hole configuration.

An obvious candidate to search for another $\nu(9/2[404])$ occurrence is the ^{97}Sr nucleus, the $N = 59$ isotone of ^{99}Zr, which has a very similar pattern of the near-yrast excitations to that observed in ^{99}Zr [4]. While investigating the $\nu(9/2[404])$ level in ^{99}Zr, we have also searched for an analogous excitation in ^{97}Sr. A characteristic signature of such a level is its isomerism, caused by the K-forbiddeness of the depopulating transitions. In ^{97}Sr an isomeric level with $T_{1/2} = 0.43(3)\,\mu$s has been found at 830.8 keV already some time ago [5,6]. The level has been tentatively assigned spin $11/2^-$, based on systematics. This level decays to the $7/2^+$ level at 308.1 keV via the 522.7 keV transition, analogous to the 786.8 keV transition from the $\nu(9/2[404])$, 1038.8 keV isomer in ^{99}Zr. Assuming that the 522.7 keV transition has the same character as that of the 786.8 keV transition, and rescaling the partial half-life for the 786.8 keV decay, $T_{1/2}(768.8) = 186(35)$ ns, with the factor $(786.8/522.7)^3$ (we neglect an $E2$ contribution) one obtains the expected partial half-life for the 522.7 keV decay of $T^{\rm ex}_{1/2}(522.7) = 635(120)$ ns. This estimate is less than two standard deviations from the observed half-life of the 830.8 keV isomer in ^{97}Sr, for which

[a] e-mail: urban@fuw.edu.pl

only the 522.7 keV decay branch is known. Therefore the 830.8 keV level in ^{97}Sr could be the $K = 9/2$, $9/2^+[404]$ neutron-hole excitation.

Despite these indications, our search for the $\nu(9/2[404])$ band in ^{97}Sr was unsuccessful, probably due to experimental limitations and contaminations in gamma spectra, as will be discussed in detail in sect. 3. In the mean time another group has studied the ^{97}Sr nucleus in search of the $\nu(9/2[404])$ excitation [7]. They report that the 830.8 keV isomer (their energy is 829.8 keV) indeed corresponds to the $\nu(9/2[404])$ excitation although they report the deformation for this configuration significantly lower than observed in ^{99}Zr. Their results will be disussed in detail further in the text, while here we only note that in ref. [7] no experimental data were presented to support the $I^\pi = 9/2^+$ spin and parity assignment to the 830 keV isomeric level.

The authors of ref. [7] aimed to verify the presence of the $\nu(9/2[404])$ excitation in the $A \sim 100$ region by finding another case. However, the association of the new band in ^{97}Sr with the $\nu(9/2[404])$ configuration is based on the similarity of this band to the $K = 9/2$ band in ^{99}Zr. One needs, therefore, to find another case of the $\nu(9/2[404])$ excitation in the region, with well documented spin and parity.

One expects that the addition of two nucleons does not change significantly the position of the Fermi level and the observed schemes of single-particle levels. Indeed, the analogous $9/2^+[404]$ proton-hole excitation is observed in a number of the $Z = 51$ and $Z = 53$ isotopes [8] (see also fig. 17 in ref. [2]) in the $A \sim 115$ mass region. By analogy one expects that the $9/2^+[404]$ neutron level, observed now in the $N = 59$ isotones, might be also seen in the $N = 61$ nuclei of the $A \sim 100$ region. We have performed a detailed study of the ^{101}Zr nucleus to search for the ν 9/2[404] excitation. In the next section we report on the identification of such a band in ^{101}Zr.

To search for the $\nu(9/2[404])$ excitation we used the data from the spontaneous fission of ^{248}Cm. In the measurement multiple, prompt-gamma coincidences were collected, using the EUROGAM 2 array of anti-Compton spectrometers. More details on experimental and data analysis techniques can be found in our previous works [3,9,10].

2 Band structure of the ^{101}Zr nucleus

The 9/2[404] neutron-hole excitation in the ^{101}Zr nucleus was first considered by Meyer *et al.* [11]. They reported in this nucleus three delayed transitions of 91.6 keV, 98.2 keV and 133.7 keV, showing a half-life of 18 ns. The isomeric level was not located, however. That finding was consistent with an earlier reporting of delayed transitions observed in the spontaneous fission of ^{252}Cf, where delayed transitions of 91.5 keV and 98.3 keV, showing half-lives of 19 ns and 21 ns, respectively, were assigned to mass $A = 101$ [12]. Another later work [13] reported delayed transitions of 91.6 keV, 98.4 keV and 133.8 keV as belonging to ^{101}Zr, though the half-lives quoted there have very large errors.

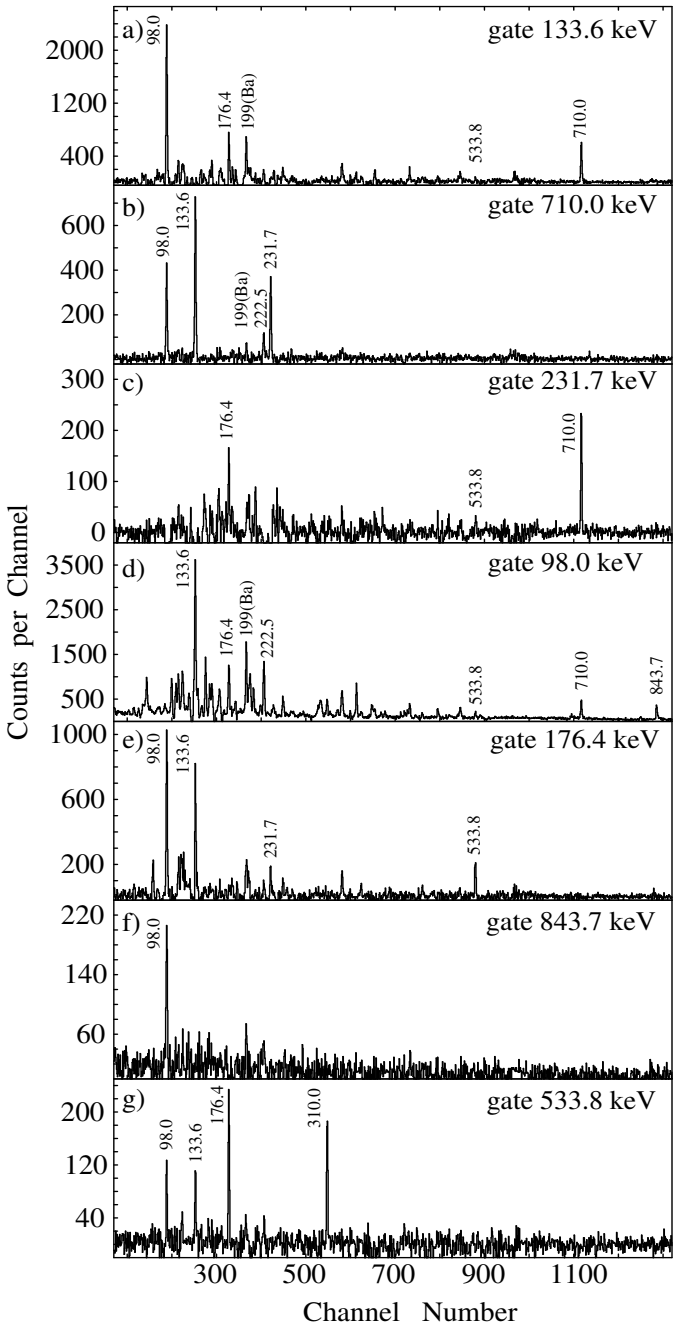

Fig. 1. Coincidence spectra of γ radiation following spontaneous fission of ^{248}Cm, gated on lines in ^{101}Zr in the dd matrix (see text for more details).

In a recent detailed investigation of ^{101}Zr populated in β^- decay of ^{101}Y [14], the authors have dismissed the 91.6 keV line as belonging to ^{101}Zr. They also could not see the 18 ns component in the 98.2 keV and 133.7 keV transitions in their data. It is interesting to note that levels with spins $I = 9/2$ are clearly populated in β^- decay of ^{101}Y [14]. The ground state of ^{101}Y, interpreted as the $5/2^+[422]$ proton configuration [15], decays to both, the $I^\pi = 9/2^+$, 467.5 keV member of the

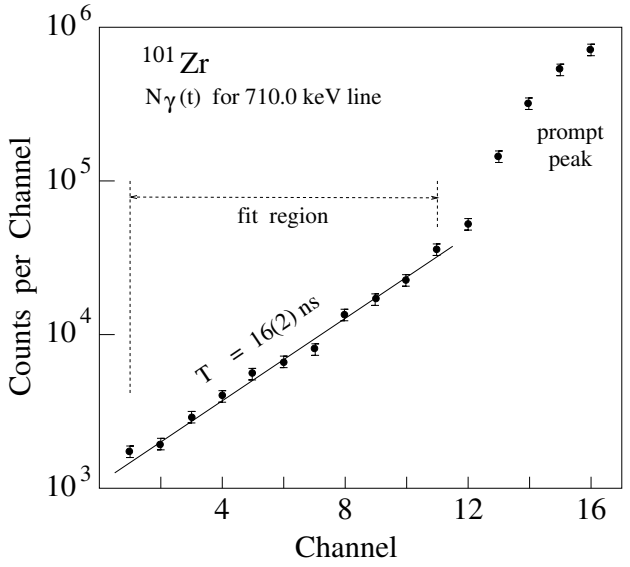

Fig. 2. Time spectrum gated on the 710.0 keV line of ^{101}Zr.

$\nu(3/2^+[411])$ ground-state band [16], and to the $I^\pi = 9/2^-$, 467.5 keV member of the $\nu(5/2^-[532])$ band [17]. The non-population of the discussed isomer in β^- decay suggests that this isomeric level either has spin higher than $I = 9/2$ or its structure is significantly different from the other two 9/2 excitations in ^{101}Zr.

In a search for this isomer, we have analysed spectra gated on a time signal. Figure 1a shows a γ-coincidence spectrum gated on the 133.6 keV line. The spectrum was cut from the so-called "delay-delay" (dd) matrix, sorted with a "delay" window (100 ns $< t <$ 300 ns) imposed on all energies sorted into the matrix. Known lines at 98.0 keV and 176.4 keV [17] are seen in the spectrum. This observation confirms that these lines are part of an isomeric cascade. A new strong line at 710.0 keV is also seen in the spectrum. A spectrum gated on this line in the dd matrix is shown in fig. 1b. The spectrum is clean and simple, characteristic of an isomeric decay. The 98.0 keV, 133.6 keV and the crossover 231.7 keV transitions are present, while the 176.4 keV transition is not seen. This indicates that the 710.0 keV transition feeds the 231.7 keV level in ^{101}Zr. The 231.7 keV gate shown in fig. 1c confirms this conclusion as the 98.0 keV and 133.6 keV lines are not seen, while the 176.4 keV and 710.0 keV lines are present in this spectrum. In spectra gated on the 98.0 keV and 176.4 keV, shown in figs. 1d and e, respectively, besides the known 98.0 keV, 133.6 keV and 176.4 keV lines, new lines at 843.7 keV and 533.6 keV are seen (the latter is also present in figs. 1a and c). Spectra gated on these new lines are shown in figs. 1f and g, respectively, confirming that the 843.7 keV transition feeds the 98.0 keV level and the 533.8 keV transition feeds the 408.1 keV level in ^{101}Zr. The new 533.8 keV, 710.0 keV and 843.7 keV transitions define a new level in ^{101}Zr at 941.8 keV. Since there are no common, new lines in the spectra gated on these transitions in the dd matrix, the 941.8 keV level is likely to be an isomer.

A time spectrum, gated on the 710.0 keV decay branch of the 941.8 keV level, is shown in fig. 2. The spectrum shows a slope corresponding to the half-life of the 941.8 keV level. The prompt component is due to prompt contaminants of the 710 keV line from other fission products. The half-life of the 941.8 keV level, deduced from the time spectrum shown in fig. 2, is $T_{1/2} = 16(2)$ ns. To obtain this value, we used the analysis methods and calibrations described in ref. [4]. The obtained half-life agrees with the $T_{1/2} = 18$ ns value reported in ref. [11].

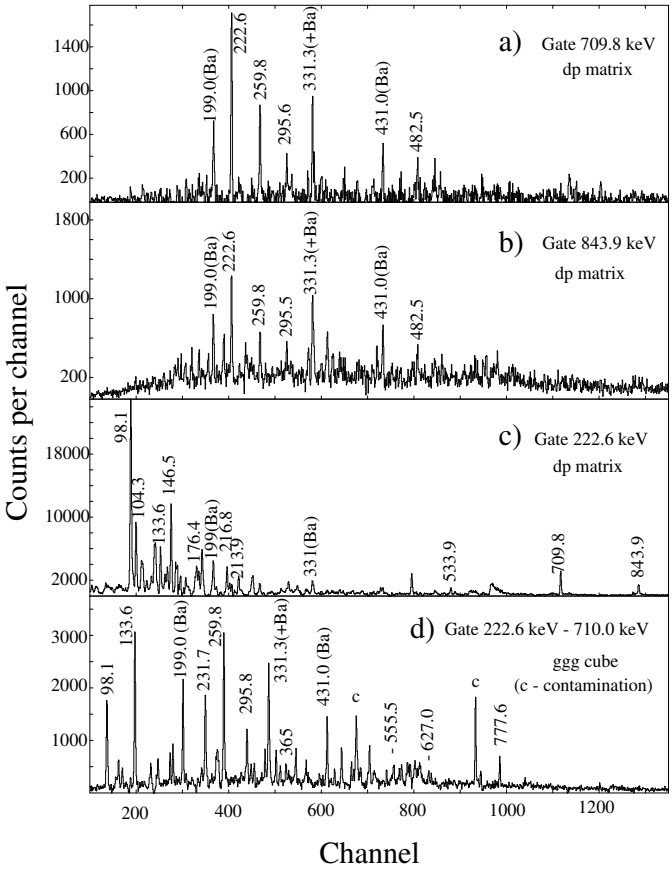

Fig. 3. Coincidence spectra of γ radiation following the fission of ^{248}Cm, gated on lines of the new band in ^{101}Zr (see text for more details).

To search for transitions feeding the 941.8 keV isomer we have analysed spectra from the so-called "delayed-prompt" (dp) matrix sorted with a "delayed" time window (100 ns $< t <$ 300 ns) on the "d" axis and a "prompt" time window ($t <$ 60 ns) on the "p" axis of the dp matrix. A spectrum gated on the 710.0 keV line on the "delayed" axis of the dp matrix, displayed in fig. 3a, reveals prompt transitions feeding the 941.8 keV level. One can see new lines at 222.6 keV, 259.8 keV and 295.6 keV in this spectrum. In an analogous spectrum gated on the 843.7 keV line on the "delay" axis of the dp matrix, shown in fig. 3b, these new lines can be seen as well. A spectrum gated on the new, 222.6 keV line on the "prompt" axis of the dp matrix, shown in fig. 3c, contains the 98.0, 133.6, 176.4, 231.7, 533.8 710.0 and 843.7 keV lines corresponding to the decay of the 941.8 keV isomeric level.

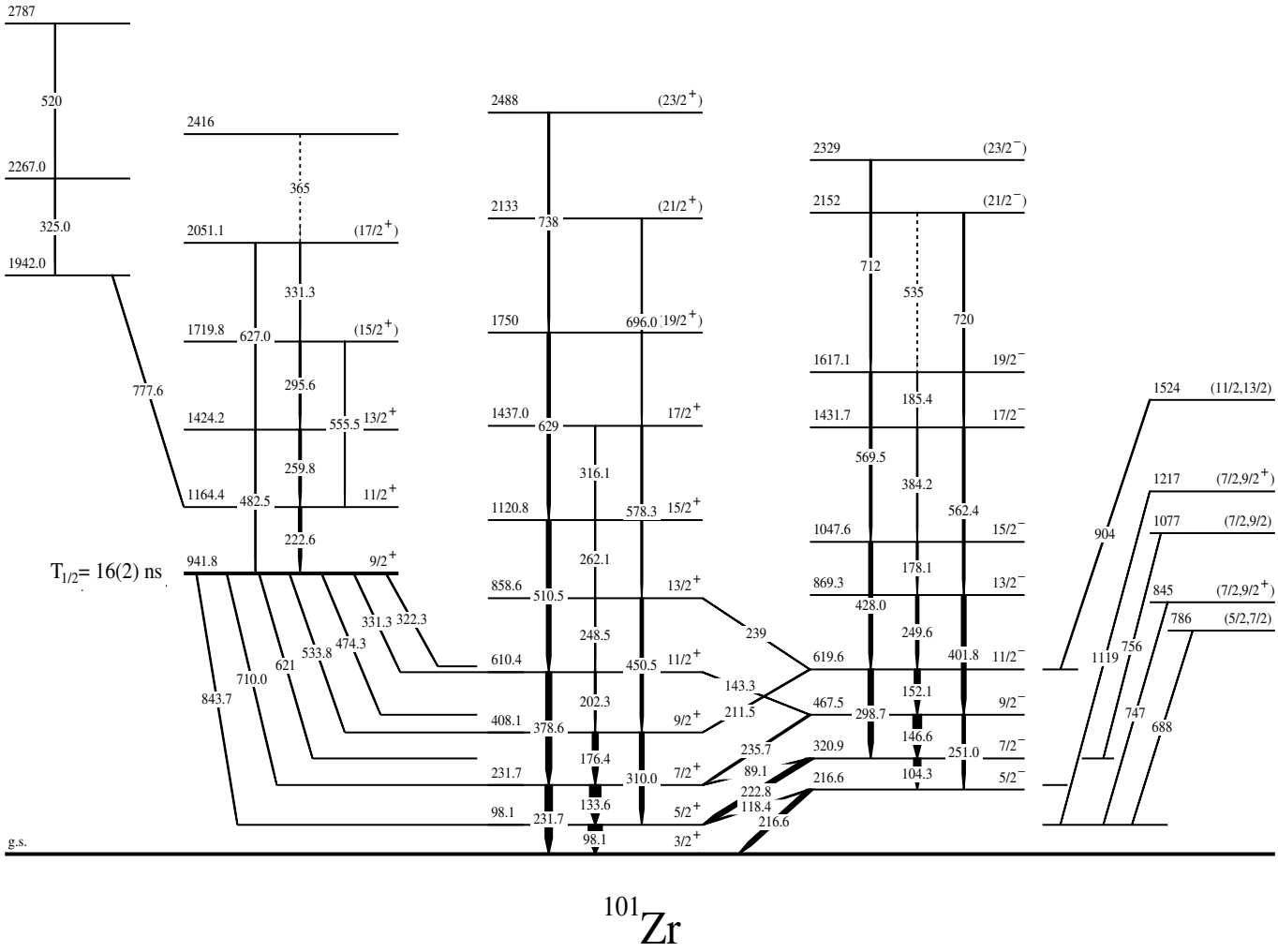

^{101}Zr

Fig. 4. Level scheme of ^{101}Zr, as obtained in this work.

Finally, we have analysed gated spectra from the so-called $\gamma\gamma\gamma$ cube, sorted with full time window ($0 < t < 300$ ns). The spectrum shown in fig. 3d, double gated on the 222.6 keV and 710.0 keV lines in the cube, shows the 259.6 keV, 295.6 keV and 331.3 keV lines. We tentatively add to this list the 365 keV transition. Further gating on triple-gamma coincidence data revealed four more decay branches of the 941.8 keV level (621 keV, 474.3 keV, 331.3 keV and 322.3 keV) and two more transitions above it (325.0 keV and 520 keV).

The above energy and time coincidence relations indicate the presence of an isomeric level at 941.8 keV in ^{101}Zr. The isomeric level with its feeding and depopulating transitions is shown in fig. 4, where we also show other excitations and gamma transitions in ^{101}Zr observed in our data, which are briefly reported below.

The $3/2^+$, ground-state band and the band on top of the $5/2^-$, 216.6 keV level in ^{101}Zr were established up to the $17/2^+$, 1437.0 keV level and the $19/2^-$, 1617.1 keV level, respectively, in a study of prompt gamma-rays following the spontaneous fission of ^{248}Cm [17]. In our work we confirm all the levels and transitions reported in ref. [17] and add, apart from the 941.8 keV configuration, 10 new levels. These are five new levels in the two bands mentioned above and five non-yrast levels, shown on the right-hand side of fig. 4, which do not form any band.

In ref. [17] spins were proposed tentatively based on the expected single-particle configurations in ^{101}Zr. Important new experimental information, added by the β^- decay study [14], is firm spin and parity assignment to the low-energy excitations in ^{101}Zr, up to the $9/2^-$, 467.5 keV level. We have used this information to extend spin and parity assignments further up the bands based on angular correlation data for transitions in ^{101}Zr, obtained using the methods of ref. [18] and shown in table 1.

The angular correlation data from table 1 are consistent with the spin and parity assignments reported in refs. [14,17]. Considering the stretched quadrupole character of the 231.7 keV, 310.0 keV, 378.6 keV, 450.5 keV, 510.5 keV and 578.3 keV transitions, we assigned spins in the ground-state band, as shown in fig. 4, assuming that spins in the band are growing with increasing excitation energy, as commonly observed for levels populated in the spontaneous fission. For the levels at

Table 1. Angular correlations for cascades of two consequtive gamma transitions in the ^{101}Zr nucleus.

E_γ-E_γ (keV)-(keV)	A_2/A_0	A_4/A_0
98.1-310.0	−0.10(1)	−0.04(2)
104.3-298.7	−0.07(1)	0.04(2)
133.6-378.6	−0.20(1)	0.07(2)
146.6-401.8	−0.10(1)	0.04(2)
152.1-428.0	−0.11(2)	0.05(2)
176.4-450.0	−0.13(2)	0.01(2)
178.1-401.8	−0.24(3)	0.02(4)
202.3-310.0	−0.07(1)	0.04(2)
213.8-378.6	0.10(1)	−0.08(2)
222.8-298.7	−0.05(2)	0.00(2)
222.6-710.0	0.11(2)	0.03(3)
248.5-378.6	−0.06(2)	−0.06(2)
249.6-298.7	−0.19(2)	−0.04(2)
251.0-401.8	0.04(2)	0.02(4)
259.8-222.6	0.13(2)	−0.04(3)
261.1-450.0	−0.09(3)	0.08(4)
298.7-428.0	0.11(2)	0.06(2)
310.0-450.0	0.10(1)	0.02(2)
316.1-510.5	−0.22(3)	0.07(4)
378.6-510.0	0.06(1)	0.01(1)
428.0-298.7	0.09(1)	−0.03(2)
450.0-310.0	0.06(1)	0.03(2)
510.5-202.3	−0.01(2)	−0.07(2)
555.5-222.6	−0.12(3)	0.16(4)
562.4-401.8	0.10(2)	0.15(4)
569.5-428.0	0.08(2)	0.06(2)
578.3-450.0	0.13(2)	−0.01(3)
629-510.5	−0.01(2)	0.00(2)
710.0-133.6	0.33(4)	−0.03(5)
710.0-231.7	−0.15(4)	−0.02(5)
777.6-222.6	0.23(4)	−0.01(5)
777.6-325.0	0.40(3)	0.08(3)
843.7-98.1	−0.08(5)	0.12(7)

Table 2. Branching ratios for levels in the ^{101}Zr nucleus.

Excited level (keV)	Transition energy (keV)	Transition intensity (rel. units)
216.6	118.4	0.13(1)
	216.6	1.00(5)
231.7	133.6	1.00(5)
	231.7	0.41(3)
320.9	89.1	0.014(2)
	104.3	1.00(5)
	222.8	0.094(5)
408.1	176.4	0.88(4)
	310.0	1.00(5)
467.5	146.6	1.00(5)
	235.7	0.16(1)
	251.0	0.27(2)
610.4	143.2	0.10(3)
	202.3	0.30(4)
	378.6	1.00(7)
619.6	152.1	1.00(5)
	211.5	0.07(2)
	298.7	0.91(5)
858.6	239	0.05(2)
	248.5	0.45(3)
	450.0	1.00(5)
869.3	249.6	1.00(6)
	401.8	0.95(5)
941.8	322.3	0.13(3)
	331.3	0.17(3)
	474.3	0.74(5)
	533.8	0.29(2)
	621	0.06(2)
	710.0	1.00(5)
	843.7	0.54(4)
1047.6	178.1	0.34(3)
	428.0	1.00(5)
1120.8	262.1	0.52(8)
	510.5	1.00(13)
1424.2	259.8	1.00(6)
	482.5	0.42(9)
1431.7	384.2	0.34(3)
	562.4	1.00(6)
1437.0	316.1	0.20(4)
	578.3	1.00(6)
1617.1	185.4	0.26(5)
	569.5	1.00(8)
1719.8	295.6	1.00(16)
	555.5	0.38(8)
2051.1	331.3	1.00(6)
	627.0	0.25(8)

1750 keV, 2133 keV and 2488 keV the assignment is tentative, suggested by the regular, rotational character of the band. Similarly, the stretched quadrupole character of the 251.0 keV, 298.7 keV, 401.8 keV, 428.0 keV, 562.4 keV and 569.5 keV transitions indicates spins in the band on top of the $5/2^-$, 216.6 keV level, as shown in fig. 4. The assignments to the 2152 keV and 2329 keV levels are tentative, based on the fact that the 712 keV and 720 keV transitions fit the rotational pattern of the in-band transitions. To the new levels, shown on the right-hand side of fig. 4, we make tentative spin assignments, which are based on the observed decay patterns and the assumption that fission populates predominantly levels close to the yrast line.

The most important conclusion drawn from the obtained angular correlations concerns the spin and parity assignment to the 941.8 keV, isomeric level. The correlation for the 710.0 keV-231.7 keV cascade indicates the $\Delta I \leq 1$ multipolarity of the 710.0 keV transition, considering the stretched, quadrupole character of the 231.7 keV transition. This is consistent with the dipole-dipole and dipole-quadrupole correlations observed for the 710.0 keV-133.6 keV and 133.6 keV-378.6 keV cascades, respectively. The above observations set an upper limit of 9/2 for the spin of the 941.8 keV isomeric level. The angular correlation for the 843.7 keV-98.0 keV pair, characteristic of a quadrupole-dipole cascade, is also consistent with this limit and indicates spin $I = 9/2$ for the 941.8 keV isomer.

We could not determine angular correlations for other transitions depopulating the 941.8 keV isomer either due to contaminations from the complementary Ba isotopes or

because of their low intensities. The observation of these decays helps, however, to fix spin and parity of the isomer. The observation of the 322.3 keV and 331.3 keV transitions to the $11/2^-$, 619.6 keV and $11/2^+$, 610.4 keV states, respectively, rules out both, $I^\pi = 7/2^+$ and $I^\pi = 7/2^-$ spin and parity assignments for the 941.8 keV level, since in either case one of the transitions would be $M2$, while the other an $E2$. The single-particle estimate of the half-life for an $M2$ transition of such energy is of the order of 10^4 ns while for an $E2$ transition it is of the order of 1 ns. Table 2 shows branching ratios from the levels in ^{101}Zr, as obtained in this work. The branching ratios for the 941.8 keV level can be used to find partial half-lives for transitions depopulating the isomer. They are shown in table 3. Partial half-lives of 361 ns and 276 ns for the 322.3 keV and 331.3 keV transitions, respectively, differ significantly from values expected for an $M2$ or $E2$ transition of about 330 keV. Possible solutions are the $E1$ and $M1 + E2$ multipolarities for the two discussed transitions, respectively. Such an assignment is consistent with spin $I = 9/2$ for the 941.8 keV level. Similar arguments allow the rejection of spins lower than 7/2. From the evidence presented above we conclude that the spin of the 941.8 keV isomeric level in ^{101}Zr is $I = 9/2$.

To find the parity of the isomeric level, we note that one observes the 843.7 keV quadrupole transition from the 941.8 keV isomer to the $5/2^+$ level at 98.1 keV, whilst there is no decay to the $5/2^-$ level at 216.6 keV. The partial half-life for the 843.7 keV decay of the 941.8 keV isomer is 87(12) ns, while the lower limit for the partial half-life of the (unobserved) 725 keV transition to the 216.6 keV level is about 5000 ns. Single-particle half-life estimates are 3 ns (0.05 ns) for an $M2$ ($E2$) transition of 843 keV and 7 ns (0.1 ns) for an $M2$ ($E2$) transition of 725 keV. If the parity of the 941.8 keV isomer is negative, then the partial half-life for the 843.7 keV transition is consistent with an $M2$ multipolarity assignment for this transition, assuming a typical hindrance of 20 for an $M2$ transitions. In this case, however, the non-observation of an $E2$ decay to the 216.6 keV level is surprising. It would require hindrance higher than 5×10^4 to explain the absence of an $E2$ transition with an energy of 725 keV. If, on the other hand, one assigns positive parity to the isomer, then the experimental data can be explained, assuming that there is a hindrance of 1.7×10^3 to the 843.7 keV, $E2$ decay and a hindrance of 0.7×10^3 to the unobserved, 752 keV, $M2$ decay, the two values being of the same order.

A possible explanation of the nature of the 941.8 keV isomer is that it is caused by K isomerism. The K value of the isomer should be as high as 9/2 to account for the 87 ns partial half-life corresponding to the 843.7 keV, $E2$ decay branch and the observed branching ratios. Assuming, for instance, $K = 7/2$ for the 941.8 keV level allows an unhindered $E2$ transitions to the $K = 3/2$, ground-state band. In such a case, $M1$ components of the 710.0 keV and 533.8 keV transitions have a $n = 1$ degree of K forbiddeness, and can be neglected. The relative probabilities for the 843.7 keV $E2$ and 710.0 keV transitions, calculated from Alaga rules are $B^{\rm cal}(E2, 843.7\,{\rm keV})/B^{\rm cal}(E2, 710.0\,{\rm keV}) = 2.5$. This is significantly different from the experimental branching ratio $B^{\rm exp}(E2, 843.7\,{\rm keV})/B^{\rm exp}(E2, 710.0\,{\rm keV}) = 0.23(4)$ and allow, therefore, the rejection of the $K = 7/2$ hypothesis.

Table 3. Properties of the transitions deexciting the 941.8 keV isomer in ^{101}Zr. T_W is the single-particle Weisskopf estimate, H is the hindrance and n is the degree of forbiddeness, as defined in ref. [19]. For the 331.3, 533.8 and 710.0 keV transitions both, $M1$ and $E2$ multipolarities were considered.

E_γ (keV)	Mult.	$T^{\rm part.}_{1/2}$ (ns)	T_W (s)	H	$\frac{\log H}{n}$
322.3	$E1$	361(85)	9.3×10^{-15}	$3.9\ 10^7$	
331.3	$M1$	276(63)	6.4×10^{-13}	$4.3\ 10^5$	2.8
331.3	$E2$	276(63)	5.0×10^{-9}	55	1.8
474.3	$E1$	63(8)	2.9×10^{-15}	$2.2\ 10^7$	
533.8	$M1$	162(22)	1.5×10^{-13}	$1.1\ 10^6$	3.0
533.8	$E2$	162(22)	4.6×10^{-10}	352	2.5
621	$E1$	782(260)	1.3×10^{-15}	$5.9\ 10^8$	
710.0	$M1$	47(6)	6.5×10^{-14}	$7.2\ 10^5$	2.9
710.0	$E2$	47(6)	1.1×10^{-10}	427	2.6
843.7	$E2$	87(12)	4.7×10^{-11}	1851	3.3

In table 3 partial half-lives for the decay branches of the isomer are compared to their single-particle, Weisskopf estimates taking $I^\pi = 9/2^+$ and $K = 9/2$ for the 941.8 keV level. For all the decay branches a considerable hindrance (H) is observed. Following the procedure of ref. [19] we calculated a hindrance per degree of forbiddeness, $(\log H)/n \approx 2$ for the $E2 + M1$, 843.7 keV, 710.0 keV and 533.8 keV decays to the $K = 3/2$ ground-state band. The values obtained are consistent with the $(\log H)/n$ values observed for $M1$ and $E2$ transitions in this region [19, 20], supporting the K isomerism of the 941.8 keV level.

Summarizing, to explain the observed decay properties of the 941.8 keV isomer we propose that this level is a $K = 9/2$ isomer with spin and parity $I^\pi = 9/2^+$. The only neutron orbital in this region characterised by such quantum numbers is the ν 9/2[404], recently observed in ^{99}Zr [3]. Therefore we propose that this is the configuration of the 941.8 keV isomer. This is another observation of the ν 9/2[404] orbital in the $A \sim 100$ region, which confirms our previous report [3] on the presence of this excitation in the region.

On top of the 941.8 keV isomer we have found a band of four transitions of 222.6 keV, 259.8 keV, 295.6 keV, 331.3 keV and a tentative 365 keV transition. The first three transitions from this list are $\Delta I = 1$ in character as can be deduced from the angular correlation data. The angular correlations for the 843.7 keV-222.6 keV and 710.0 keV-222.6 keV cascades are consistent with a quadrupole multipolarity for the 843.7 keV and dipole multipolarities for the 710.0 keV and 222.6 keV transitions. Further up the band, angular correlations for the 222.6 keV-259.8 keV and 259.8 keV-295.6 keV pairs are consistent with $\Delta I = 1$ character of all the three transitions. Since the 331.3 keV transition and the tentative

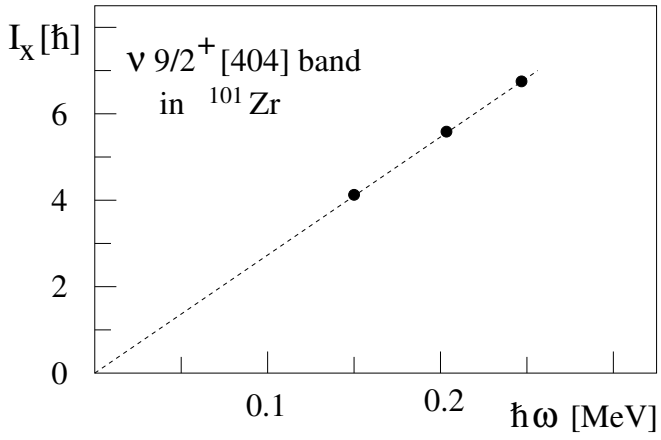

Fig. 5. Aligned angular momentum for the new $K = 9/2$ band based on the $9/2^+$, 941.8 keV isomer in ^{101}Zr.

365 keV transition follow the very regular rotational pattern of the band we assume that they belong to this structure and are also of $\Delta I = 1$ character.

It is expected that, as observed in ^{99}Zr [3], the 9/2[404] orbital in ^{101}Zr will show a very small alignment. In fig. 5 we have plotted the total aligned angular momentum, $I_x = \sqrt{(I+1/2)^2 - K^2}$ for the new band and fitted a linear dependence to the experimental points, shown as the dashed line in fig. 5. Experimental points fit nearly exactly the line, which is characteristic of a rigid rotor. The moment of inertia of a nucleus, usually parametrized as $J = J_0 + J_1\omega^2$, has in such case a vanishing $J_1\omega^2$ component. Therefore the I_x can be represented as $I_x = J\omega + i$, where the $J\omega$ term corresponds to the collective rotation and i is the aligned angular momentum of the valence particle. For the new band in ^{101}Zr, however, the $J_1\omega^2$ is neglected and $I_x = J_0\omega + i$ is represented by the straight line in fig. 5. Since this line goes very close to the zero point, it is evident that the value of alignment i is close to zero, as expected for the $K = 9/2$, $9/2^+[404]$ neutron orbital.

The 1164.4 keV level of the new band is fed by the 777.6 keV transition from 1942.0 keV level. Angular correlations for the 777.6 keV-222.6 keV pair are characteristic of a dipole-dipole or quadrupole-quadrupole cascade. Since the 222.6 keV transition has been shown to be a dipole, we conclude that the 777.6 keV transition has a dipole character. On top of the 1942.0 keV level a cascade of two transitions, 325.0 keV and 520 keV, is observed. Angular correlations for the 777.6 keV-325.0 keV cascade are consistent with a dipole character for both the 325.0 keV and 777.6 keV transitions.

3 The 9/2[404] band in ^{97}Sr

The 829.8 keV isomer in ^{97}Sr decays by the cascade of 522.0 keV, 140.8 keV, and 167.0 keV transitions [7]. Figure 1 of ref. [7] shows a complex spectrum, double gated on the 522.0 keV and 167.0 keV lines. The 205.9 keV, 239.6 keV, 272.5 keV and 304.0 keV transitions, seen in this spectrum, were assigned to the band built on top of the 829.8 keV isomer in ^{97}Sr [7].

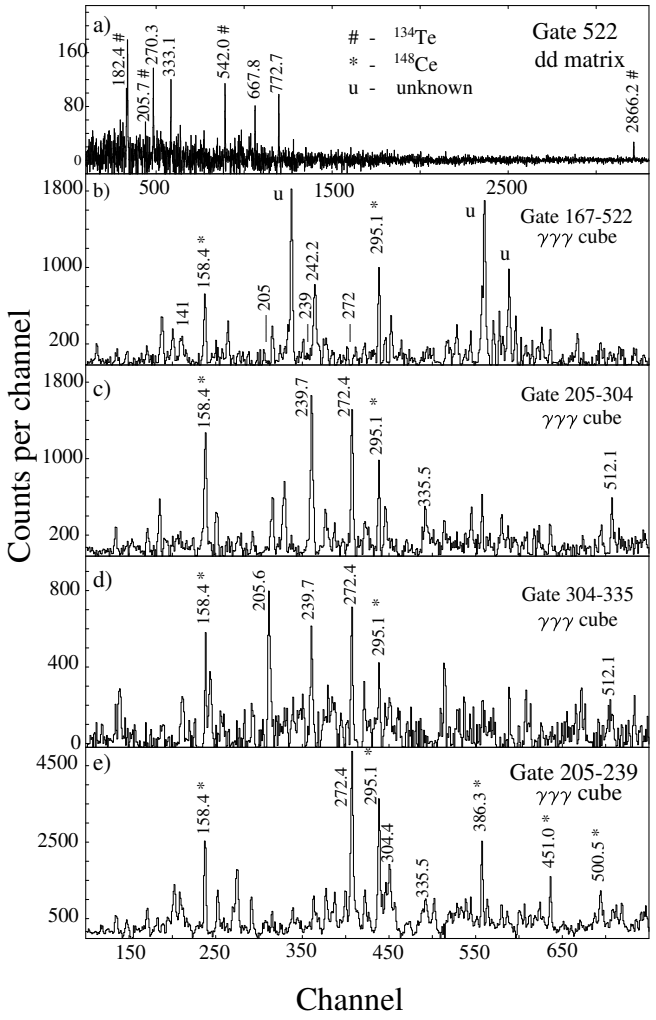

Fig. 6. Coincidence spectra of γ radiation following the fission of ^{248}Cm, gated on lines in ^{97}Sr.

The search for the 9/2[404] band on top of the 830 keV level in ^{97}Sr in our experiment is greatly complicated by the fact that in our data the 522 keV line is rather complex, even in time-gated spectra. The main effect in connection with this line, seen in our data, is due to the 522.1 keV transition in a cascade depopulating the $T_{1/2} \approx 20$ ns isomer at 5806 keV in the ^{134}Te isotope [21,22].

In fig. 6a we show the 522 keV gate cut from the dd matrix. One sees there transitions depopulating the 5806 keV isomer in ^{134}Te and other unidentified lines. The 167 keV and 141 keV transitions from ^{97}Sr are probably hidden in the background and cannot be identified. A spectrum double gated on the 522 keV and 167 keV transitions in a $\gamma\gamma\gamma$ histogram is shown in fig. 6b. This spectrum has more counts in it and is more selective. One can see here a weak line at 141 keV. However, the transitions in the 9/2[404] band, shown in fig. 1 of ref. [7], are not seen. A possible reason for this discrepancy is the lack of cross-coincidences

through the 830 keV isomer in our data. In our measurement the electronic time window for accepting events was about 300 ns. Consequently, the observation of isomers with half-lives longer than that is strongly reduced. The time window used in ref. [7] was about 1 microsecond, which could significantly enhance the observation of long-living isomers. This argument holds if the half-life of the 830 keV isomer is around the 515 ns value, reported in ref. [6]. However, in ref. [7] a two times shorter half-life of $T_{1/2} = 265$ ns is now reported for the 830 keV isomer, which complicates the story. In our data we should be able to "see through" such an isomer. Another measurement to verify the new, 265 ns half-life of the 830 keV isomer, reported in ref. [7], would be valuable.

Though the connection of the new band, reported in ref. [7], to the levels below the 830 keV isomer is not seen in our data, we do observe prompt coincidences between the lines in this band. In fig. 6c we show a spectrum double gated on the 205 keV and 304 keV lines, reported in ref. [7] as members of the band on top of the 830 keV isomer. In this spectrum lines at 239.7 keV, 272.5 keV and 512.1 keV are seen, which is consistent with the gamma cascade reported in ref. [7] (note that there is no sign of the 522 keV line). The lines in fig. 6c are quite intense, with about 4000 counts in the highest peak. Double gates set on other lines of the band are also consistent with the coincidences above the isomer, reported in ref. [7]. In addition we see the 335.5 keV line, which corresponds to the next, $\Delta I = 1$ transition in the discussed band. In the spectrum double gated on the 304 keV and 335 keV lines, shown in fig. 6d, the 239.7 keV, 272.4 keV and 272.4 keV lines can be seen, confirming the assignment of the 335.5 keV line to the new band in ^{97}Sr.

We can also see prompt coincidences between the new band and the gamma transitions in the complementary fission fragments. In fig. 6e the 158.4, 295.1, 386.3 and 451.0 keV lines, corresponding to transitions in the ground-state band of ^{148}Ce, the most abundant fission-fragment partner to ^{97}Sr, are present. This observation supports the assignments of the new band to ^{97}Sr. Summarizing, we observe a gamma cascade of 205.6 keV, 239.7 keV, 272.4 keV, 304.4 and the 335.5 keV transitions and assign this band to the ^{97}Sr nucleus, confirming the observation and the assignment of this band reported in ref. [7]. Some facts remain unexplained though, as for instance the lack of "across the isomer" coincidences which might be expected, considering the new, shorter half-life of the 830 keV isomer. Though there is no experimental data to assign spin and parity to the 830 keV isomer, we cautiously assume that the new band corresponds to the 9/2[404] excitation because of its similarity to the 9/2[404] band in ^{99}Zr. In our data the coincidences below the isomer indicate that the energy of the isomer is 830.7 keV.

4 Discussions and conclusions

The enriched data on the $\nu 9/2^+[404]$ configuration in the $A \sim 100$ region allows us to discuss various subjects related to these excitations. Below, we will compare the properties of these bands which have now been seen in three nuclei. We will then discuss their role in the onset of deformation in the region and finally will mention some related problems which are not yet solved.

4.1 Properties of $\nu(9/2^+[404])$ bands

It is interesting to ask what is the deformation of the ^{101}Zr nucleus in the band based on the 941.8 keV isomer. One can estimate the quadrupole moment for the $9/2^+[404]$ band, where $g_K = -0.255\ \mu_N$ [3], from gyromagnetic ratios in this band. Experimental gyromagnetic ratios, $|g_K - g_R|/Q_0$ were derived for levels in the $K = 9/2$ band in ^{101}Zr, taking branchings from table 2 and following the calculation procedure described in ref. [23]. The values obtained in this way are 0.102(15), 0.15(2) and 0.26(5) for the $13/2^+$, $15/2^+$ and $17/2^+$ band members, respectively. The weighted average, $\langle g^{\rm exp}\rangle = 0.127(14)$, used to estimate the quadrupole moment from the relation $Q_0 = |g_K - g_R|/\langle g^{\rm exp}\rangle$, assuming $g_R = 0.2\ \mu_N$ [23] and taking $g_K = -0.255\ \mu_N$, yields $Q_0 = 3.6(4)$ eb, a similar value to that obtained for the $9/2^+[404]$ band in ^{99}Zr. From the quadrupole moment one can estimate the deformation parameter, β_2, using the standard formula $\beta_2 = (91.7Q_0)/(ZA^{2/3})$ [24]. Taking $Q_0 = 3.6(4)$ eb we calculate $\beta_2 = 0.38(4)$ for the $9/2^+[404]$ band in ^{101}Zr. This result is close to the $\beta_2 = 0.41(3)$ value obtained for the $9/2^+[404]$ band in ^{99}Zr [3] (in the present work we have improved this value, which now reads $\beta_2 = 0.420(25)$, determining more accurately the branching for the 2105.4 keV, $17/2^+$ level: $I_\gamma(313.8\,\text{keV}) = 1.00(8)$, $I_\gamma(597.7\,\text{keV}) = 0.38(10)$).

In view of this similarity, the quite different Q_0 and the resulting β_2, reported for the $9/2^+[404]$ band in ^{97}Sr [7], calls for an explanation if the interpretation of the band should stay. We note that ^{97}Sr and ^{99}Zr have exactly the same neutron cores in the $9/2^+[404]$ bands, and from fig. 3 of ref. [7] one can see that the $9/2^+[404]$ bands in ^{97}Sr and ^{99}Zr have nearly identical kinematic moments of inertia. We also note that the $9/2^+[404]$ bands in ^{97}Sr and ^{99}Zr have a very similar branching ratio for the $13/2^+$ level [3,7]. Since other parameters of the bands are also the same, while the Q_0 in ^{97}Sr reported in ref. [7] is quite different from Q_0 values found in ^{99}Zr and ^{101}Zr, we have checked the calculations of ref. [7]. Using branching ratios from table 1 of ref. [7] we obtained $|g_K - g_R|/Q_0$ values of 0.104(4), 0.161(10) and 0.206(14) for the $13/2^+$, $15/2^+$ and $17/2^+$ band members, respectively. The recalculated values are in good agreement with those obtained for ^{99}Zr and ^{101}Zr, while they are different from those reported in ref. [7] (we note that, if misread, the formulas of ref. [23], used to calculate $|g_K - g_R|/Q_0$, give results reported in ref. [7]). The weighted average of the new $|g_K - g_R|/Q_0$ values in ^{97}Sr, $\langle g^{\rm exp}\rangle = 0.118(4)$, gives quadrupole moment of $Q_0 = 3.86(13)$ eb, which converts [24] to $\beta_2 = 0.441(15)$ for the $9/2^+[404]$ band in ^{97}Sr. This result is consistent with the β_2 values obtained for ^{99}Zr and ^{101}Zr.

For the disputed band in ^{97}Sr we were able to extract branching ratios from our ^{248}Cm fission data. The

Table 4. Branching ratios and experimental gyromagnetic ratios for levels in the 9/2[404] band in ^{97}Sr, as obtained in this work.

Level spin	$E_\gamma(^{97}\mathrm{Sr})$ (keV)	$I_\gamma(^{97}\mathrm{Sr})$ (relative)	$[(g_K - g_R)/Q_0]_{\exp}$ ^{97}Sr
13/2	239.7	3.0(2)	0.108(10)
	445.4	1.0(4)	
15/2	272.4	1.8(2)	0.124(10)
	512.1	1.0(1)	
17/2	304.4	1.2(1)	0.130(20)
	576.7	1.0(1)	

Table 5. Rotational properties of the $\nu(9/2[404])$ bands.

	^{97}Sr	^{99}Zr	^{101}Zr
Q_0	3.9(2)	3.8(3)	3.6(4)
β_2	0.44(2)	0.42(3)	0.38(4)
J_0(MeV)	28.0	26.8	25.8
J_0/J_{rig}	0.88	0.79	0.76

results are shown in table 4. The weighted average of experimental gyromagnetic ratios, $\langle g^{\exp} \rangle = 0.118(7)$, yields quadrupole moment $Q_0 = 3.86(23)$ eb, and the deformation parameter, $\beta_2 = 0.441(26)$. These values are identical to those obtained from the branchings reported in ref. [7]. The similarity to the Q_0 values, obtained for $9/2^+[404]$ bands in ^{99}Zr and ^{101}Zr, supports the interpretation of the band discussed here in ^{97}Sr as the strongly deformed $9/2^+[404]$ neutron-hole configuration.

In table 5 we compare rotational properties of the three known $\nu 9/2^+[404]$ bands. The J_1 moment is in all three cases negligible, *i.e.* the bands correspond to a nearly rigid rotor, as also seen in the last line of table 5, where we compare experimental moments of inertia to the corresponding rigid-body values.

In fig. 7 we show schemes of the three bands and mark the positions of the $3/2^+$, $3/2^-$ and $5/2^-$ deformed configurations in the discussed nuclei. The $9/2^+[404]$ is positioned about 200 keV above the $3/2^+$ and $3/2^-$ levels in ^{97}Sr and this distance increases with increasing neutron and proton number. Consequently, the half-lives of the $9/2^+[404]$ isomers become shorter. Using this trend as a rough guide, one expects that the possible ν $9/2^+[404]$ bands in ^{101}Mo and ^{103}Mo will be placed higher in energy and may have shorter half-lives. This could make them more difficult to detect.

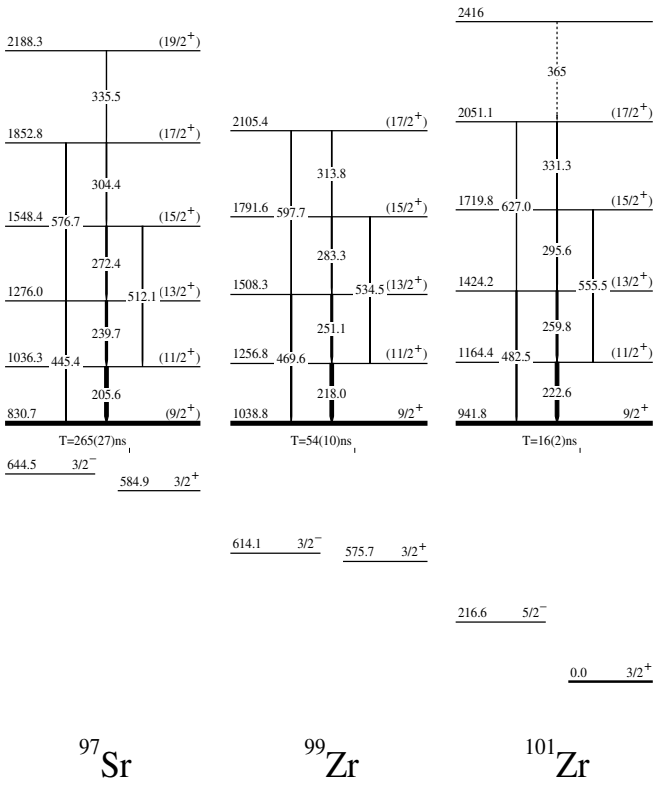

Fig. 7. The $\nu 9/2^+[404]$ bands in ^{97}Sr, ^{99}Zr and ^{101}Zr.

4.2 The onset of deformation in the A $\sim$ 100 region

In fig. 8, which is an updated version of fig. 9 from ref. [4], we compare β_2 values for the three known $9/2^+[404]$ bands in ^{97}Sr, ^{99}Zr and ^{101}Zr with β_2 values found for other bands in strontium and zirconium isotopes of the $A \sim 100$ region. Included are new β_2 values for the deformed $3/2^+$ and $5/2^-$ bands in ^{101}Zr, obtained from Q_0 moments measured [25] for the $3/2^+$, g.s. band and the $5/2^-$, 216.6 keV

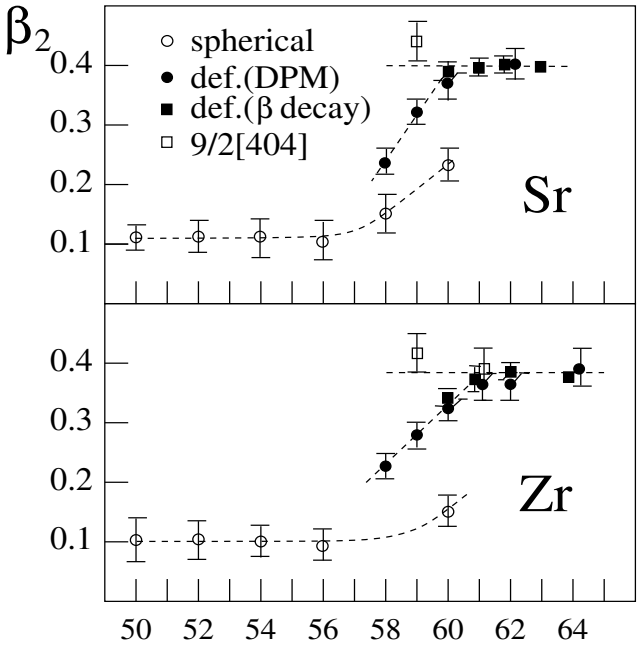

Fig. 8. Deformation of various configurations in Sr and Zr isotopes. Lines are drawn to guide the eye. The data are from this work and refs. [3,14,27–37]. See text for more explanations.

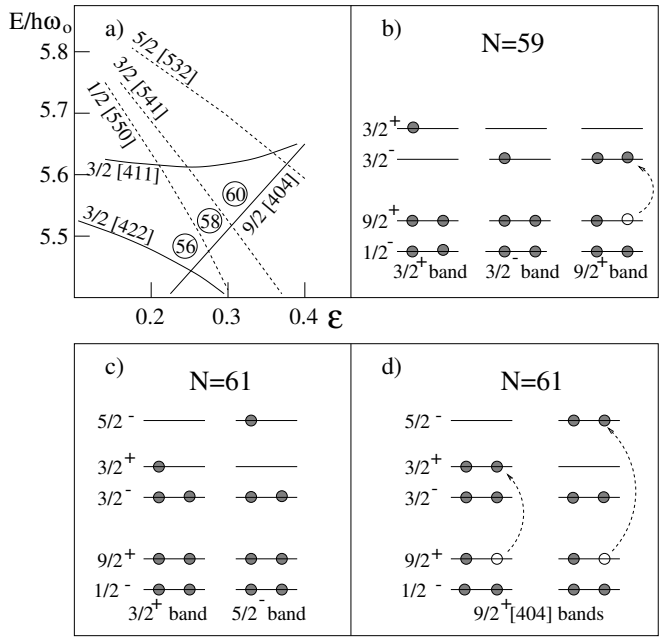

Fig. 9. a) Portion of the Nilsson neutron levels (after ref. [17]) and b)-d) schematic representations of deformed configurations in Sr and Zr isotopes.

band using the Doppler Profile method (DPM) [26], and applying the relation $\beta_2 = (91.7Q_0)/(ZA^{2/3})$ [24]. We also show β_2 values deduced in other works [14,27–37] from the properties of low-energy levels populated in β^- decay, for which half-lives were measured (if more than one value was available for a given nucleus, we took their average).

In the past the possibility of a sudden onset of the deformation at $N = 59$ was considered (see, *e.g.*, fig. 10 in ref. [36]). In our previous work [4] we have pointed out that at medium spins the deformation increases rather gradually. There are indications, both experimental (see fig. 8) and theoretical [38], that in the zirconium isotopes this change takes place over a neutron range $58 \leq N \leq 62$. The observation of the $\nu 9/2^+[404]$ configurations in this region offers now more insight into this effect.

As seen in fig. 8, in Sr and Zr isotopes with $N = 59$ neutrons, one observes three different deformations. The nearly spherical configurations based on the $s_{1/2}$, $d_{5/2}$ and $g_{7/2}$ neutron levels (open circles), the deformed configurations, based on the $\nu(3/2^+[411])$, $\nu(3/2^-[541])$ and $\nu(5/2^-[541])$ Nilsson orbitals (filled circles —values obtained using the DPM method [26]; filled squares —values obtained in β^- decay studies) and the strongly deformed $\nu(9/2^+[404])$ configurations (open squares). It is evident that at $N = 59$ the deformation of the $\nu(3/2^+[411])$ and $\nu(3/2^-[541])$ configuration is half-way to the saturation limit. On the other hand, the deformation of the $\nu(9/2^+[404])$ configurations at $N = 59$ is as high as the saturation limit for the deformed configurations.

Paradoxically, slowing down of the deformation onset may be due to the presence at the Fermi level of the same $\nu(9/2^+[404])$ orbital, which produces the spectacular, large deformation at $N = 59$. In fact, the $\nu(9/2^+[404])$ neutron-hole bands, observed now in ^{97}Sr, ^{99}Zr and ^{101}Zr, "simulate" the situation of what would have happened if the 9/2[404] orbital was not present. This is illustrated schematically in fig. 9.

Figure 9a shows a portion of a Nilsson diagram for neutrons in the $N \sim 60$ region, taken from ref. [17]. When the number of neutrons reaches $N = 58$, the $\nu(1/2^-[550])$ deformation driving orbital is filled and the deformation appears. It corresponds to moving towards larger ϵ values in fig. 9a. The increase of the deformation stops when the strongly upsloping $\nu(9/2[404])$ level is encountered at a moderate ϵ value.

At $N = 59$, the odd neutron can be placed either on the $3/2^-[541]$ or the $3/2^+[411]$ orbital. The deformation is larger than at $N = 58$ but the $\nu(9/2[404])$ orbital still limits the deformation. This is illustrated in fig. 9b where we show schematically the population of orbitals, corresponding to the deformed bands with spins $3/2^-$ and $3/2^+$, respectively, observed at $N = 59$. In both bands the core has the same two pairs of neutrons, one pair in the deformation driving $\nu(1/2^-[550])$ orbital and the other pair in the upsloping $\nu(9/2^+[404])$ orbital, working against the deformation. It is only when one neutron of the $\nu(9/2^+[404])^2$ pair is promoted to the $3/2^-[541]$ orbital and couples to the other neutron in that orbital, that the situation changes dramatically, as first described by Kleinheinz *et al.* [2] in the lanthanide region for an analogous $\nu(11/2^-[505])$ orbital. The corresponding population of levels is shown on the right-hand side of fig. 9b. Now the "spectator" neutron is in the $9/2^+[404]$ orbital and the core contains two pairs of neutrons in the deformation driving, $1/2^-[550]$ and $3/2^-[541]$ orbitals, respectively. This configuration corresponds to the strongly deformed $\nu(9/2^+[404])$ bands seen in the ^{97}Sr and ^{99}Zr nuclei. Since the two most important deformation driving orbitals (and no $9/2^+[404]$ neutrons) are in the core here, this configuration has its deformation at the saturation limit already at $N = 59$.

At $N = 60$ the deformation increases further because the $\nu(3/2^-[541])$ orbital is filled. Consequently, the core has now the same deformation driving orbitals as in the strongly deformed $\nu(9/2^+[404])$ bands at $N = 59$. But there is also a pair of neutrons in the $\nu(9/2^+[404])$ orbital, which may still limit the deformation increase. Such a pair must be near the Fermi level at $N = 60$ in zirconium isotopes, as indicated by the observation of the $\nu(9/2^+[404])$ bands both in ^{99}Zr and ^{101}Zr. Therefore, in ^{100}Zr the deformation is still below the saturation limit. This can be seen in fig. 8 and is also indicated by the different excitation energies in the ground state bands of ^{100}Zr and ^{102}Zr. In contrast, in strontium isotopes the deformation is saturated already at $N = 60$, as can be seen in fig. 8. This is confirmed by similar excitation energies in the ground state bands in ^{98}Sr and ^{100}Sr, which are one of the best examples of identical bands [35,39].

At present we cannot explain why the deformation sets in faster in strontium than in zirconium isotopes. It is an

interesting question whether this difference could be related to the position of the $\nu(9/2^+[404])$ orbital in the Nilsson diagram. In fig. 7 one can see that the position of the $\nu(9/2^+[404])$ orbital relative to the deformed configurations differs significantly in Sr and Zr nuclei.

It is possible that the saturation of the deformation in ^{98}Sr is a "normal" phenomenon while in ^{100}Zr one observes another effect, slowing down the onset of deformation. We note that in molybdenum isotopes, the deformation change is even slower than in zirconiums and that this trend continues with the increasing proton number (see, for instance, fig. 1a. of ref. [40]).

At $N = 61$ the situation is analogous to that at $N = 59$. In ^{101}Zr one sees two deformed bands with the odd neutron in the $3/2^+[411]$ and $5/2^-[532]$ orbitals, respectively. Their configurations are illustrated in fig. 9c. The newly observed, $9/2^+[404]$ band in ^{101}Zr most likely corresponds to one of the two configurations shown in fig. 9d. One may see in fig. 8 that deformations of the $3/2^+[411]$, $5/2^-[532]$ and $9/2^+[404]$ bands are nearly the same. This suggests that the $\nu(9/2^+[404])^2$ pair in the core does not influence the deformation at $N = 61$.

4.3 Further studies

With the presence of the 9/2[404] orbital now well established one can discuss possible further studies in the field of "9/2[404] spectroscopy". These may involve the search for further examples of the 9/2[404] neutron excitations in odd-N nuclei; in two-quasiparticle excitations of even-even nuclei; in proton-neutron excitations of odd-odd nuclei; and in three-quasiparticle excitations of odd-Z nuclei of the $A \sim 100$ region. Some results have already been reported. The examples are the $11/2^-$ and $17/2^-$ three-quasiparticle isomers in the ^{99}Y nucleus, with the proposed $\pi 5/2[422] \otimes \{\nu(9/2[404])\nu(3/2[411])\}_{3^+,6^+}$ configuration [19], or the corresponding two-quasiparticle $K^\pi = 3^+$ isomer in ^{98}Sr with $\{\nu(9/2[404])\nu(3/2[411])\}_{3^+}$ configuration [20]. We note that in ^{98}Sr one expects also the $K^\pi = 6^+$ coupling of the two orbitals, as seen in ^{99}Y.

An interesting feature of ^{101}Zr, which will need further studies, is the side feeding to the 9/2[404] band shown in fig. 4. The 1942.0 keV level decays to the $11/2^+$ level of the 9/2[404] band rather than to the $11/2^+$ level of the ground-state band, which is lower in energy. This observation suggests structural similarity between the 1942.0 keV level and the 9/2[404] band and a significant hindrance of the decay to the $11/2^+$ member of the ground-state band. This could be explained assuming that the 1942.0 keV level has $K \geq 9/2$. We note that, in principle, the 9/2[404] configuration in ^{101}Zr can be produced in more than one way. As illustrated in fig. 9d, this could be done by promoting the 9/2[404] neutron either to the $3/2^+[411]$ or to the $5/2^-[532]$ orbital. The $3/2^+$ and the $5/2^-$ excitations in ^{101}Zr are close in energy, as can be seen in fig. 4. Therefore, in principle, one may expect two 9/2[404] bands with similar core deformations. At present we are not able to answer if the 1942.0 keV, 2267.0 keV and 2787 keV levels belong to such a hypothetical, second 9/2[404] band. Another possibility is that these levels belong to the signature partner band.

The work was supported by the French-Polish IN2P3-KBN collaboration No. 01-100, by the UK EPSRC under grant no. GRH71161 and by the US Dept. of Energy under contract No. W-31-109-ENG-38. The authors are also indebted, for the use of ^{248}Cm to the Office of Basic Energy Sciences, US Dept. of Energy, through the transplutonium element production facilities at the Oak Ridge National Laboratory.

References

1. P. Kleinheinz, R.K. Sheline, M.R. Maier, R.M. Diamond, F.S. Stephens, Phys. Rev. Lett. **32**, 68 (1974).
2. P. Kleinheinz, A.M. Stefanini, M.R. Maier, R.K. Sheline, R.M. Diamond, F.S. Stephens, Nucl. Phys. A **283**, 189 (1977).
3. W. Urban, J.A. Pinston, T. Rząca-Urban, A. Złomaniec, G. Simpson, J.L. Durell, W.R. Phillips, A.G. Smith, B.J. Varley, I. Ahmad, N. Schulz, Eur. Phys. J. A **16**, 11 (2003).
4. W. Urban, J.L. Durell, A.G. Smith, W.R. Phillips, M.A. Jones, B.J. Varley, T. Rząca-Urban, I. Ahmad, L.R. Morss, M. Bentaleb, N. Schulz, Nucl. Phys. A **689**, 605 (2001).
5. J. Genevey *et al.*, *ENAM98 Exotic Nuclei and Atomic Masses Bellaire, Michigan, USA, 1998*, AIP Conf. Proc. **455**, 694 (1998).
6. E. Monnand, J.A. Pinston, F. Schussler, J.B. Battistuzzi, K. Kamada, H. Lawin, K. Sistemich, B. Pfeiffer, CEA-N-2176 (1980) p. 20.
7. J.K. Hwang, A.V. Ramayya, J.H. Hamilton, D. Fong, C.J. Beyer, P.M. Gore, Y.X. Luo, J.O. Rasmussen *et al.*, Phys. Rev. C **67**, 054304 (2003).
8. A.K. Gaigalas, R.E. Shroy, G. Schatz, D.B. Fossan, Phys. Rev. Lett. **35**, 555 (1975).
9. W. Urban, J.L. Durell, W.R. Phillips, A.G. Smith, M.A. Jones, I. Ahmad, A.R. Barnett, M. Bentaleb, S.J. Dorning, M.J. Leddy, E. Lubkiewicz, L.R. Morss, T. Rząca-Urban, R.A. Sareen, N. Schulz, B.J. Varley, Z. Phys. A **358**, 145 (1997).
10. W. Urban, W. Kurcewicz, A. Nowak, T. Rząca-Urban, J.L. Durell, M.J. Leddy, M.A. Jones, W.R. Phillips, A.G. Smith, B.J. Varley *et al.*, Eur. Phys. J. A **5**, 239 (1999).
11. R.A. Meyer *et al.*, Brookhaven National Laboratory, Report BNL 51778 (1983) p. 321.
12. W. John, F.W. Guy, J.J. Wesolowski, Phys. Rev. C **2**, 1451 (1970).
13. R.G. Clark, L.E. Glendenin, W.L Talbert jr., IAEA-SM-174/86, 221 (1986).
14. G. Lhersonneau, H. Gabelmann, M. Liang, B. Pfeiffer, K.-L. Kratz, H. Ohm, the ISOLDE Collaboration, Phys. Rev. C **51**, 1211 (1995).
15. R.F. Petry, J.D. Goulden, F.K. Wohn, J.C. Hill, R.L. Gill, A. Piotrowski, Phys. Rev. C **37**, 2704 (1988).
16. K. Shizuma, H. Ahrens, J.P. Bocquet, N. Kaffrell, B.D. Kern, H. Lawin, R.A. Meyer, K. Systemich, G. Tittel, N. Trautmann, Z. Phys. A **315**, 65 (1984).
17. M.A.C. Hotchkis, J.L. Durell, J.B. Fitzgerald, A.S. Mowbray, W.R. Phillips, I. Ahmad, M.P. Carpenter, R.V.F. Janssens, T.L. Khoo, E.F. Moore, L.R. Morss, Ph. Benet, D. Ye, Nucl. Phys. A **530**, 111 (1991).

18. M.A. Jones, W. Urban, W.R. Phillips, Rev. Sci. Instrum. **69**, 4120 (1998).
19. R.A. Meyer, E. Monnand, J.A. Pinston, F. Schussler, I. Ragnarsson, B. Pfeiffer, H. Lawin, G. Lhersonneau, T. Seo, K. Sistemich, Nucl. Phys. A **439**, 510 (1985).
20. G. Lhersonneau, B. Pfeiffer, R. Capote, J.M. Quesada, H. Gabelmann, K.-L. Kratz, the ISOLDE Collaboration, Phys. Rev. C **65**, 024318 (2002).
21. C.T. Zhang, P. Bhattacharyya, P.J. Daly, R. Broda, Z.W. Grabowski, D. Nisius, I. Ahmad, T. Ishii, M.P. Carpenter, L.R. Morss, W.R. Phillips, J.L. Durell, M.J. Leddy, A.G. Smith, W. Urban, B.J. Varley, N. Schulz, E. Lubkiewicz, M. Bentaleb, J. Blomqvist, Phys. Rev. Lett. **77**, 3743 (1996).
22. S.K. Saha, C. Constantinescu, P.J. Daly, P. Bhattacharyya, C.T. Zhang, Z.W. Grabowski, B. Fornal, R. Broda, I. Ahmad, D. Seweryniak, I. Wiedenhöver, M.P. Carpenter, R.V.F. Janssens, T.L. Khoo, T. Lauritsen, C.J. Lister, P. Reiter, Phys. Rev. C **65**, 017302 (2001).
23. H. Mach, F.K. Wohn, M. Moszyński, R.L. Gill, R.F. Casten, Phys. Rev. C **41**, 1141 (1990).
24. S. Raman, C.H. Malarkey, W.T. Milner, C.W. Nestor jr., P.H. Stelson, At. Data Nucl. Data Tables **36**, 1 (1987).
25. A.G. Smith *et al.*, to be published.
26. A.G. Smith, J.L. Durell, R. Phillips, M.A. Jones, M. Leddy, W. Urban, B.J. Varley, I. Ahmad, M. Bentaleb, A. Guessous, E. Lubkiewicz, N. Schulz, R. Wyss, Phys. Rev. Lett. **77**, 1711 (1996).
27. R.C. Jared, H. Nifenecker, S.G. Thompson, *Proceedings of the Third Symposium on Physics and Chemistry Fission, IAEA Rochester, NY* (IAEA-SM-174 Vienna, 1974) p. 211.
28. F.K. Wohn, J.C. Hill, C.B. Howard, K. Systemich, R.F. Petry, R.L. Gill, H. Mach, A. Piotrowski, Phys. Rev. C **33**, 677 (1986).
29. H. Ohm, M. Liang, G. Molnar, K. Systemich, Z. Phys. A **334**, 519 (1989).
30. H. Mach, M. Moszyński, R.L. Gill, F.K. Wohn, J.A. Wigner, J.C. Hill, G. Molnár, K. Systemich, Phys. Lett. B **230**, 21 (1989).
31. G. Lhersonneau, B. Pfeiffer, K.-L. Kratz, H. Ohm, K. Systemich, S. Brant, V. Paar, Z. Phys. A **337**, 149 (1990).
32. H. Ohm, G. Lhersonneau, K. Systemich, B. Pfeiffer, K.-L. Kratz, Z. Phys. A **327**, 483 (1987).
33. G. Lhersonneau, H. Gabelmann, N. Kaffrell, K.-L. Kratz, B. Pfeiffer, Z. Phys. A **332**, 243 (1989).
34. G. Lhersonneau, H. Gabelmann, B. Pfeiffer, K.-L. Kratz, Z. Phys. A **352**, 293 (1995).
35. G. Lhersonneau, H. Gabelmann, N. Kaffrell, K.-L. Kratz, B. Pfeiffer, K. Heyde, the ISOLDE Collaboration, Z. Phys. A **337**, 143 (1990).
36. H. Mach, F.K. Wohn, G. Molnár, K. Sistemich, J.C. Hill, M. Moszyński, R.L. Gill, W. Krips, D.S. Brenner, Nucl. Phys. A **523**, 197 (1991).
37. M.A.C. Hotchkis, J.L. Durell, J.B. Fitzgerald, A.S. Mowbray, W.R. Phillips, I. Ahmad, M.P. Carpenter, R.V.F. Janssens, T.L. Khoo, E.F. Moore, L.R. Morss, Ph. Benet, D. Ye, Phys. Rev. Lett. **64**, 3123 (1990).
38. J. Skalski, P.-H. Heenen, P. Bonche, Nucl. Phys. A **559**, 221 (1993).
39. F. Schussler, J.A. Pinston, E. Monnand, A. Moussa, G. Jung, E. Koglin, B. Pfeiffer, R.V.F. Janssens, J. van Klinken, Nucl. Phys. A **339**, 415 (1980).
40. F.K. Wohn, J.C. Hill, F.R. Petry, H. Dejbakhsh, Z. Berant, R.L. Gill, Phys. Rev. Lett. **51**, 873 (1983).